Transactions on the Built Environment vol 19, © 1996 WIT Press, www.witpress.com, ISSN 1743-3509

Substructure system identification: reduced-order models

R. Craig, E. Blades
Department of Aerospace Engineering and Engineering Mechanics, The University of Texas at Austin, Austin, TX 78712, USA

Abstract

When a complex structural system must be analyzed for its response to dynamic excitation, some form of substructure coupling method, or component mode synthesis (CMS) method, is usually employed. It is generally necessary to perform some form of vibration test to validate the separate substructure math models, which are then coupled together for the system analysis. When such tests are performed, it is important to give special attention to the way that the substructure is supported and the way that it is excited. A new substructure system identification algorithm, which produces a linear, viscous-damped, reduced-order physical model (i.e., M, C, and K), is described in this paper, and the results of numerical simulations used to test the proposed new algorithm are presented. Of particular interest is the comparison between the results obtained by using the ordinary least-squares (OLS) method and those based on the total least-squares (TLS) method.

1 Introduction

When a structural system (e.g., the Space Shuttle Orbiter plus payloads) must be analyzed for its response to dynamic excitation, some form of substructure coupling method, or component mode synthesis (CMS) method, is usually employed (e.g., Craig & Bampton,[1] NASA[2]). It is frequently necessary to perform some form of vibration test to validate the separate substructure math models, which are then coupled together for the system analysis. When such tests are performed, it is important to give special attention to the way that the substructure is supported and the way that it is excited (e.g., Mühlbauer, Troidl, & Dillinger,[3] Admire, Tinker, & Ivey,[4] Chung, Sernaker, & Peebles[5]).

A proposed new substructure system identification (SSID) method[6] produces a linear, viscous-damped, reduced-order physical model (i.e., M, C, and K), with all substructure interface-DOF entries included. In the vibration test used to acquire frequency response functions (FRFs), all interface degrees of freedom where the substructure is connected to the carrier structure are either subjected to active excitation or are supported by a test stand with the reaction forces measured. Although several methods have been proposed in the past for so-called direct parameter identification of mass, damping, and stiffness matrices from test data (e.g., Craig, Kurdila, & Kim,[7] Leuridan, Brown, & Allemang,[8] Balmès[9]), none has specifically addressed the identification of substructure matrices that include all of the information necessary for coupling components together.

This paper presents the results of numerical simulations used to test the SSID algorithm, with "noise" included in the simulated vibration test data. The simulations examine the algorithm's ability to identify valid reduced-order structural models using frequency response functions covering a limited frequency range. Of particular interest is the comparison between the results obtained by using the ordinary least-squares method and those based on the total least-squares method.

2 Substructure system identification theory

Assume that the substructure has viscous damping and that the total number of motion transducers (accelerometers) is at least twice the expected number of normal modes in the frequency range of interest. Every interface degree of freedom is to have a co-located force/accelerometer pair. In addition, there are to be motion sensors (accelerometers) at selected interior degrees of freedom (DOFs).

Let the equations of motion in physical coordinates and the output equation be

$$\begin{aligned} M\ddot{x} + C\dot{x} + Kx &= Dp(t) \\ y &= \ddot{x} \end{aligned} \tag{1}$$

where $x \in R^{N_x}$ is the displacement vector; $p \in R^{N_p}$ is the input force vector; $y \in R^{N_y}$ is the output measurement vector; M, C, and K are the system mass, damping, and stiffness matrices; and D is the force distribution matrix. For the present discussion, we will assume that the above N_x-degree-of-freedom model represents a reduced-order model of the structure. Let the coordinates be partitioned in the following manner:

$$x \equiv \left\{ \begin{array}{c} x_i \\ x_b \end{array} \right\} \equiv \left\{ \begin{array}{c} x_i \\ x_f \\ x_r \end{array} \right\} \tag{2}$$

where f stands for forced DOFs (i.e., DOFs where there is an active force input); r stands for reaction DOFs (i.e., interface DOFs where the tested substructure reacts against the support structure); i stands for interior DOFs (i.e., not a DOF where and active force is applied or a reaction is measured); and b stands for boundary DOFs, the combination of f-coordinates and r-coordinates. These sets of coordinates are illustrated in Fig. 1.

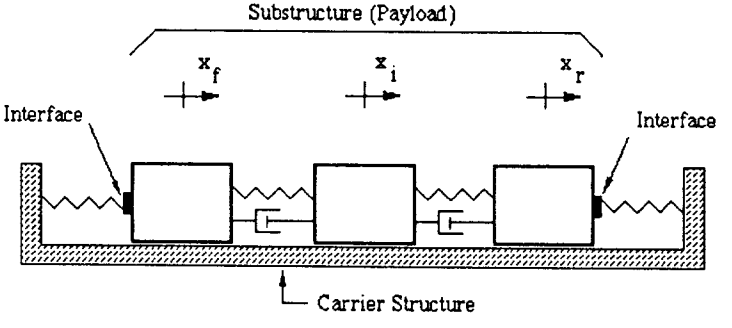

(a) Substructure model – in-service configuration.

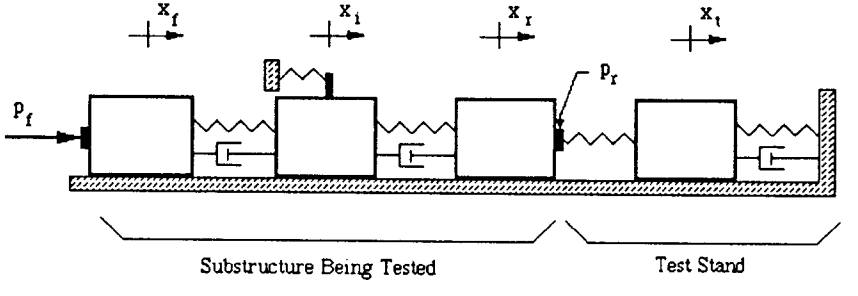

(b) Substructure model – vibration test configuration.

Figure 1: Substructure model – in-service configuration and test configuration.

Let us consider the complex frequency response of the substructure due to excitation at frequency ω_k, but with the interior DOFs force-free. Then,

$$p_k(t) \equiv \left\{ \begin{array}{c} p_f(t) \\ p_r(t) \end{array} \right\}_k = P(\omega_k) e^{j\omega_k t} \equiv \left\{ \begin{array}{c} F(\omega_k) \\ R(\omega_k) \end{array} \right\} e^{j\omega_k t} \qquad (3)$$

(From Eq. 3 onward, the vectors can be complex.) The complex displacement response can be written as

$$x_k(t) = X(\omega_k)e^{j\omega_k t} \tag{4}$$

After some manipulation, the following equation is obtained for estimating the matrices $\hat{C}$, $\hat{K}$, $\hat{D}_f$ and $\hat{D}_r$:

$$\begin{bmatrix} \hat{C} & \hat{K} & \hat{D}_f & \hat{D}_r \end{bmatrix} \begin{bmatrix} \Re\left[\frac{H_{af}}{j\omega}\right] & \Im\left[\frac{H_{af}}{j\omega}\right] \\ \Re\left[\frac{H_{af}}{-\omega^2}\right] & \Im\left[\frac{H_{af}}{-\omega^2}\right] \\ -\Re[H_{ff}] & -\Im[H_{ff}] \\ -\Re[H_{rf}] & -\Im[H_{rf}] \end{bmatrix} = \begin{bmatrix} -\Re[H_{af}] & -\Im[H_{af}] \end{bmatrix} \tag{5}$$

where

$$\hat{C} = M^{-1}C \quad , \quad \hat{K} = M^{-1}K \quad , \quad \hat{D}_f = M^{-1}D_f \quad , \quad \text{and} \quad \hat{D}_r = M^{-1}D_r \tag{6}$$

and the H matrices are measured FRF matrices. Section 3 summarizes the ordinary least-squares method and the total least-squares method, which were used for solving Eq. 5 for the examples presented in Section 4.

From the identified "hat" matrices we wish to determine the substructure matrices M, C, K, and D, especially the first three. The first step is to perform an eigensolution using the "hat" matrices identified from Eq. 5. Let $N_s \equiv 2N_x$, and define the state variable

$$z \equiv \begin{Bmatrix} x \\ \dot{x} \end{Bmatrix} \tag{7}$$

and the following state matrices:

$$\hat{A}_s = \begin{bmatrix} \hat{C} & I \\ I & 0 \end{bmatrix} \quad , \quad \hat{B}_s = \begin{bmatrix} \hat{K} & 0 \\ 0 & -I \end{bmatrix} \quad , \quad \text{and} \quad \hat{D}_s = \begin{bmatrix} \hat{D} \\ 0 \end{bmatrix} \tag{8}$$

Then the following eigenproblem is solved for the complex eigenvalues λ_r and the complex eigenvectors $\hat{\theta}_r$:

$$[\lambda_r \hat{A}_s + \hat{B}_s]\hat{\theta}_r = 0 \qquad r = 1, \ldots, N_s \tag{9}$$

To determine the system matrices M, C, and K, a mode-superposition representation of the complex frequency response can be employed. Let the state matrices A_s and B_s be defined by

$$A_s = \begin{bmatrix} C & M \\ M & 0 \end{bmatrix} \quad , \quad B_s = \begin{bmatrix} K & 0 \\ 0 & -M \end{bmatrix} \tag{10}$$

It can be shown that orthogonality holds in the following form:[6]

$$\begin{aligned} \hat{\Theta}^T A_s \hat{\Theta} &= \mathrm{diag}(\tilde{a}_r) \\ \hat{\Theta}^T B_s \hat{\Theta} &= \mathrm{diag}(\tilde{b}_r) \end{aligned} \tag{11}$$

From the solution of the following mode-superposition frequency response equation, least-squares estimates of the N_s modal parameters $\tilde{a}_r$ are obtained.

$$\left\{ \begin{array}{c} \left\{ \begin{array}{c} H_{af_1}(\omega_1) \\ \vdots \\ H_{af_1}(\omega_{N_\omega}) \end{array} \right\} \\ \vdots \\ \left\{ \begin{array}{c} H_{af_{N_f}}(\omega_1) \\ \vdots \\ H_{af_{N_f}}(\omega_{N_\omega}) \end{array} \right\} \end{array} \right\} = \left[\begin{array}{c} \left[\begin{array}{cccc} E_{11} & E_{12} & \cdots & E_{1,N_s} \\ & & \vdots & \\ E_{N_\omega,1} & E_{N_\omega,2} & \cdots & E_{N_\omega,N_s} \end{array} \right]_{f_1} \\ \vdots \\ \left[\begin{array}{cccc} E_{11} & E_{12} & \cdots & E_{1,N_s} \\ & & \vdots & \\ E_{N_\omega,1} & E_{N_\omega,2} & \cdots & E_{N_\omega,N_s} \end{array} \right]_{f_{N_f}} \end{array} \right] \left\{ \begin{array}{c} 1/\tilde{a}_1 \\ \vdots \\ 1/\tilde{a}_{N_s} \end{array} \right\} \tag{12}$$

Equation 12 is the key equation that is required for obtaining estimates of the system matrices M, C, and K. It is used to obtain least-squares estimates of the N_s modal parameters $\tilde{a}_r$. (For the simulations in Section 4, ordinary least-squares solutions and total least-squares solutions are compared.) The corresponding modal parameters $\tilde{b}_r$ can then be computed from

$$\tilde{b}_r = -\lambda_r \tilde{a}_r \qquad r = 1, \ldots, N_s \tag{13}$$

With these values of $\tilde{a}_r$ and $\tilde{b}_r$, the state matrices A_s and B_s, defined by Eqs. 10, can be computed by using Eqs. 11. Finally, the system matrices M, C, and K are obtained by referring to Eqs. 10 and extracting the appropriate partitions of the A_s and B_s matrices.

3 Least-squares equation solvers

The solutions of the systems of linear, algebraic equations, Eqs. 5 and 12, are the key mathematical steps in the substructure system identification algorithm for accurately identifying the substructure. The method of solution can have a drastic effect on the resulting identified system. The methods of solution used for the numerical simulations in Section 4 were the (ordinary) least-squares (OLS) method and the total least-squares (TLS) method. A brief description of these methods is provided here.

The least-squares method and more recent total least-squares method are mathematical modeling procedures used to solve an under-determined or over-determined system of linear equations. Both parameter identifications in Section 2, Eqs. 5 and 12, can be cast in the form

$$AX \doteq B \tag{14}$$

where A is a $m \times n$ data matrix, X is a $n \times d$ matrix of unknowns, and B is a $m \times d$ matrix of observations. The approximate sign is used to emphasize that the data (i.e., A and/or B) may be contaminated by noise. If there is no noise in the data, then Eq. 14 will be an equality. The least-squares and total least-squares methods seek solutions that minimize the error between the true system model and the measured data. The solution obtained depends on the error model and the weighting of the data used by each method. If the noise does not match the error model, a biased estimate of the solution will result. The error models assume that the errors are uncorrelated random variables with zero mean and equal variance.

Perhaps the best known method of solution for an over-determined system of linear equations is the least-squares method. For simplicity, consider the case when $d = 1$. In the classical least squares approach, the measurements of the variables in the data matrix A are assumed to be free of error, and all errors are confined to the observation vector b. A least-squares estimation could also be performed assuming that the observation vector is known exactly, but that the data matrix contains errors. The classical least-squares solution will result in an unbiased estimate if the error model is of the form

$$Ax \doteq b = \{b_0 + \Delta b\} \tag{15}$$

The classical least-squares estimate is equivalent to minimizing the sum of the squares of the differences between the elements of the measured observation vector b and an estimated observation vector $\acute{b}$. The least-squares problem seeks to minimize $\|b - \acute{b}\|_2$ where $\acute{b}$ is the orthogonal projection of b onto the range of A, $R(A)$. This amounts to perturbing the observation vector b by a minimum amount $\Delta\acute{b}$ so that $\acute{b} = b - \Delta\acute{b}$ lies in the $R(A)$. The minimum pertubation, $\Delta\acute{b}$, is the called the least-squares correction. The resulting estimation, assuming that A is of full

rank, is

$$x = (A^T A)^{-1} A^T b \tag{16}$$

The main assumption made in the classical least-squares estimation is that errors only occur in the observation vector b, and that the data matrix A is noise-free. However, this assumption is frequently unrealistic: sampling errors, modeling errors, instrument errors and human errors may imply inaccuracies of the data matrix A as well. This will cause the least-squares solution to a yield biased estimate.

The total least-squares method was developed to provide estimates from a linear system of equations where both the data matrix A and the observation matrix B are assumed to contain errors.[10] The error model for the total least-squares method is of the form

$$[A_0 + \Delta A]X \doteq \{B_0 + \Delta B\} \tag{17}$$

The total least-squares problem is formulated by rewriting Eq. 14 as a homogenous, linear system of equations:

$$[A; B] \begin{bmatrix} X \\ -I \end{bmatrix} \doteq 0 \tag{18}$$

The total least-squares formulation seeks to minimize the Frobenius norm $\|[A; B] - [\hat{A}; \hat{B}]\|_F$, subject to $\hat{B} \in R(\hat{A})$, where $\hat{A}$ and $\hat{B}$ are the total least-squares approximations of A and B required to obtain a compatible set. The Frobenius norm, $\|\cdot\|_F$, is a measure of the size of a matrix; it is similar to the 2-norm, which measures the size or length of a vector.

The solution to this system of homogenous linear equations is orthogonal to the row space of the augmented data matrix, that is, the solution lies in the null space of the augmented data matrix. The nullspace of a matrix consists of all vectors $\hat{X}$ such that $[A; B]\hat{X} = 0$. There are numerous methods that can be used to divide the augmented data matrix into a system subspace and a null subspace, but the numerically stable singular value decomposition is the method that is most often used.

The singular value decomposition of matrix $[A; B]$ can be computed as:[11]

$$[A; B] = U\Sigma V^T = [U_1; U_2] \begin{bmatrix} \Sigma_1 & 0 \\ 0 & \Sigma_2 \end{bmatrix} \begin{bmatrix} V_{11} & V_{12} \\ V_{21} & V_{22} \end{bmatrix}^T \tag{19}$$

where U is an $m \times m$ matrix whose columns are called the left singular vectors, Σ is an $m \times (n + d)$ diagonal matrix whose elements are called the singular values, and V is an $(n + d) \times (n + d)$ matrix whose columns are called the right singular vectors. When the rank of matrix $[A; B]$ is greater than n, the set is incompatible and the last d singular values, $\sigma_{n+1}, \ldots, \sigma_{n+d}$, are not equal to zeros. To obtain a compatible set, the

rank of $[A; B]$ must be reduced to n. The best rank n approximation of $[A; B]$ is given by

$$[\hat{A}; \hat{B}] = U\hat{\Sigma}V^T$$

where the last d singular values of $\hat{\Sigma}$ are zero. These are the smallest singular values, which are due mainly to the noise in the data. The matrix $[\hat{A}; \hat{B}]$ is the minimal correction to the augmented matrix $[A; B]$. The right singular vectors corresponding to the last d singular values define the null space of the augmented matrix and form the total least-squares solution. After being properly scaled, the total least-squares solution is

$$\hat{X} = -V_{12}V_{22}^{-1} \tag{20}$$

4 Numerical example

The parallel-beam "payload simulator" in Fig. 2 will be used to illustrate the SSID system identification procedure described in Section 2. A finite element (FE) model of the simulator, reduced from 54 DOFs to the 18 z-translational DOFs, was used as the "true" system. Modal damping at a level of 2% was added to obtain a damping matrix for the FE model. The payload simulator was hung from soft springs ("bungee cords") at nodes 11, 13, 14, and 16; and was excited in the z direction at all three interface nodes: 4, 8, and 18. (Examples that employ measured reactions are given in Craig, Cutshall & Blades,[6] Craig,[12] and Craig, Blades & Cutshall.[13]) Identification of both a full-order model and a reduced-order model are illustrated.

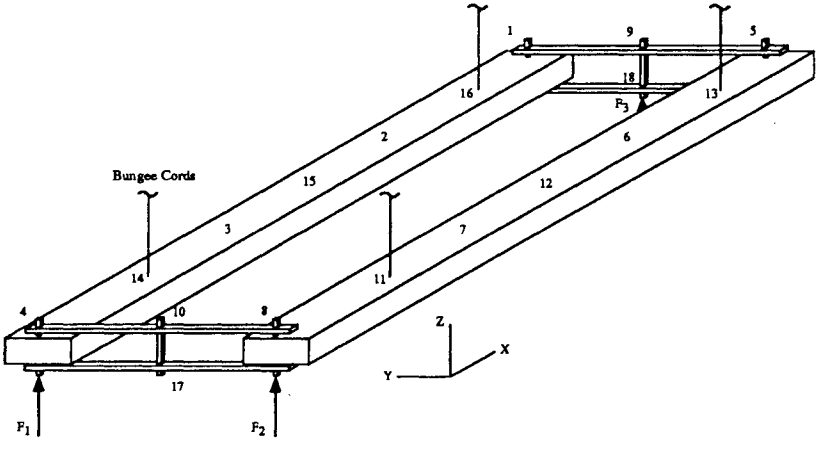

Figure 2: Payload simulator.

4.1 Identification of the full-order model

The first simulation is of the full-order model without any noise on the simulated FRF data. The SSID identification was based on 256 frequency lines uniformly spaced from 0.5 Hz to 2000 Hz. The undamped natural frequencies of the 18-DOF system, which range from 1.15 Hz to 8597 Hz, were all identified exactly (to within 7-digit accuracy), even though two of the undamped natural frequencies are well above the 2000 Hz upper limit of the FRF data. All simulations were programmed using MATLAB™[14].

Figures 3a through 3c show the percent errors in individual terms of the mass, damping, and stiffness matrices of the 18-DOF full-order model. Figure 4 shows a comparison between an exact driving-point FRF and the corresponding FRF for the identified full-order model.

4.2 Identification of reduced-order models

System identification tests of real structures are typically based on (sometimes triaxial) measurements taken at 25 to 500 nodes, whereas finite element models of the (infinite-DOF) structures are generally of the order of 1000 to 100,000 DOFs. In order to test the performance of the SSID algorithm in identifying reduced-order models, simulated tests were performed on the payload simulator by eliminating the FRF test data at four nodes (2, 3, 6, 7), reducing the system from an 18-DOF system to a 14-DOF system.

The first reduced-order simulation was run without added measurement noise in order to examine the effect of spatial filtering of the data. The SSID identification was based on simulated FRF data generated at 1021 frequency lines equally spaced at 0.5 Hz between 2 Hz and 512 Hz. Since spatial filtering to obtain a reduced-order model introduces bias error in the data, the total least-squares method was used, even though there was no random "measurement noise" added for this case. Based on the SSID-identified 14-DOF reduced-order model, twelve of the fourteen undamped natural frequencies were identified to within 0.5%. Figure 5 shows a comparison of an exact driving-point FRF and the corresponding FRF based on the SSID-identified 14-DOF reduced-order model.

Next, in order to simulate actual test conditions, noise was added to produce "measured" FRFs for a simulated 14-DOF reduced-order test. Random noise was added to the magnitude and phase of the "measured" FRFs, with the amount of noise specified in terms of the maximum percentage of the RMS magnitude of each FRF and a maximum angle error on phase. Signal averaging was employed in these simulations, just as averaging would be employed in an actual test. The two least-squares methods discussed in Sect. 3, the ordinary least-squares (OLS) method and the total least-squares (TLS) method, were used to solve the two over-determined sets of equations, Eqs. 5 and 12.

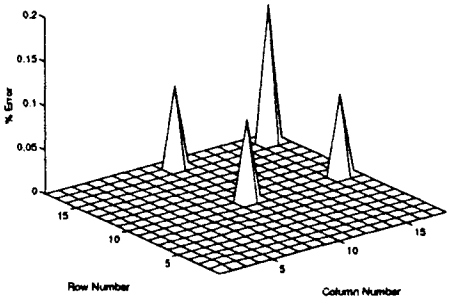

(a) Mass matrix error.

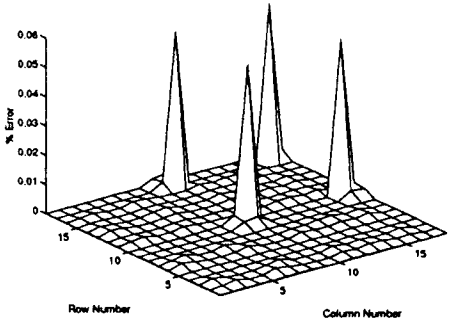

(b) Damping matrix error.

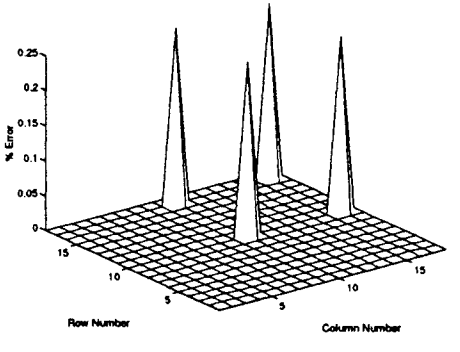

(c) Stiffness matrix error.

Figure 3: Percent errors in elements of the substructure matrices.

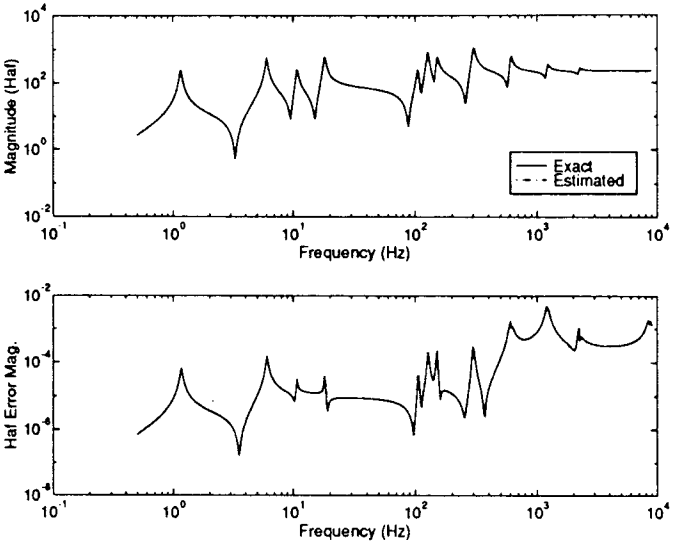

Figure 4: A driving-point FRF of the 18-DOF full-order model.

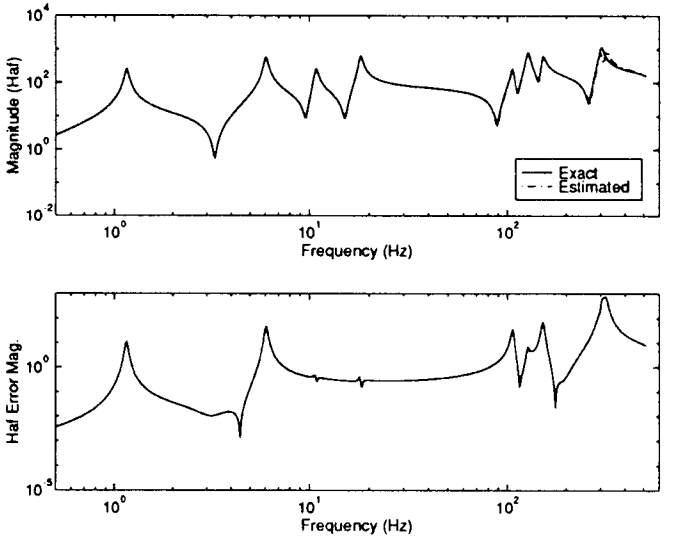

Figure 5: Exact driving-point FRF and FRF based on reduced-order SSID model (no noise).

Simulated FRF data was generated at 1021 frequency lines equally spaced at 0.5 Hz between 2 Hz and 512 Hz. For these simulations 3% amplitude noise and 3° phase noise was added to generate "measured" FRFs. These FRFs were averaged over $N = 100$ samples.

In Table 1, the natural frequencies generated from the OLS- and TLS-estimated 14-DOF M and K matrices are compared to the first fourteen exact undamped natural frequencies of the full-order (18-DOF) system and to the SSID-identified undamped natural frequencies based on noise-free (NF) FRFs.

Table 1. Natural frequencies (Hz) of 14-DOF reduced-order models.

Mode	Exact	NF	% Err	OLS	% Err	TLS	% Err
1	1.1543	1.1564	0.18	1.1360	1.58	1.3771	19.30
2	6.0384	6.0489	0.17	6.0372	0.02	5.9258	1.86
3	10.783	10.783	0.00	10.791	0.07	10.728	0.51
4	18.127	18.127	0.00	17.932	1.07	18.121	0.03
5	106.08	106.38	0.28	101.42	4.40	106.02	0.06
6	127.27	127.27	0.00	119.54	6.07	126.76	0.40
7	129.38	129.49	0.08	126.22	2.44	129.19	0.15
8	151.52	151.90	0.25	152.23	0.05	151.60	0.05
9	299.12	299.14	0.01	—	—	272.08	9.04
10	304.16	319.93	5.18	—	—	300.57	1.18
11	604.31	602.88	0.24	—	—	—	—
12	606.90	606.21	0.11	—	—	—	—
13	1212.4	—	—	—	—	—	—
14	1214.0	—	—	—	—	—	—

Figure 6a shows a comparison between an exact driving-point FRF and the corresponding FRF based on the OLS-identified reduced-order model. Figure 6b shows a comparison between an exact driving-point FRF and the corresponding FRF based on the TLS-identified reduced-order model. These results are very encouraging, since they indicate that the SSID algorithm can, indeed, be used to identify reduced-order models.

5 Conclusions; Future research

An algorithm for identifying the system matrices M, C, and K using frequency-response data that includes reaction forces between the test substructure and the test stand as well as active forces has been presented. The algorithm was tested using simulated data for an 18-DOF model of a payload simulator. With simulated noise-free data, the proposed algorithm exactly identified the full-order model and also did an excellent job of identifying a 14-DOF reduced-order model. With simulated noisy

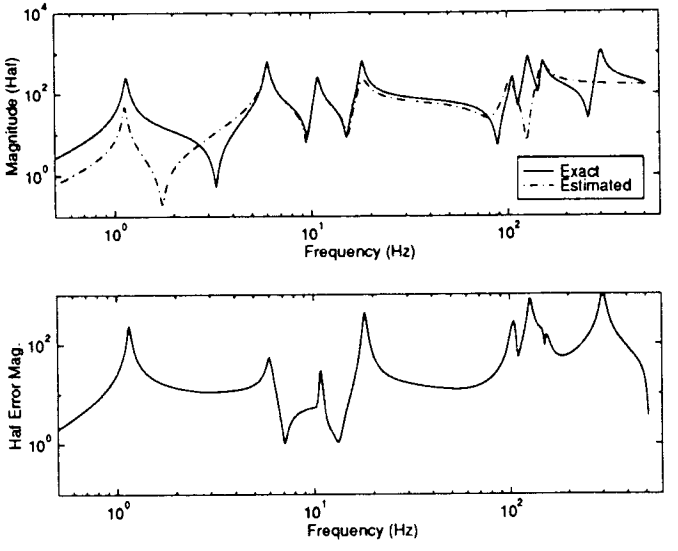

(a) Driving-point FRF based on 14-DOF OLS-identified model.

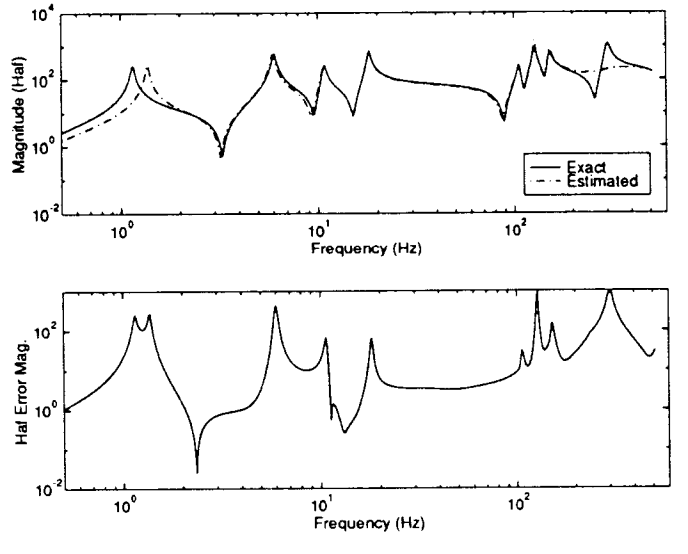

(b) Driving-point FRF based on 14-DOF TLS-identified model.

Figure 6: Frequency response functions for the 14-DOF simulated reduced-order vibration test.

data the algorithm still identified acceptable reduced-order substructure system matrices. Total least-squares solutions proved to be much better than ordinary least-squares solutions.

The relationship of reduced-order-model testing to analytical model order reduction is a subject of research at the present time. Further testing of the proposed algorithm will involve increasing the size of the simulation models, and then applying the algorithm to real test data.

Acknowledgments

The research described in this paper was conducted under Grant NAG9-670 with NASA Lyndon B. Johnson Space Center and Grant NAG8-1130 with NASA George C. Marshall Space Flight Center. The interest and support of Nancy Tengler, Michael Tinker, and Danny Coleman is greatly appreciated.

References

[1] Craig, R.R., Jr. & Bampton, M.C.C., Coupling of substructures for dynamic analysis, *AIAA Journal*, Vol. 6, No. 7, July 1968, pp. 1313-1319.

[2] *Space Shuttle Payload Design and Development, Structural/Mechanical Interfaces and Requirements*, Rev. C., NSTS 20052, Vol. 8, NASA-Lyndon B. Johnson Space Center, June 1988.

[3] Mühlbauer, K., Troidl, H. & Dillinger, S., Design, modeling and verification of a modal survey test fixture for space shuttle payloads, *Proceedings of the 10th International Modal Analysis Conference*, San Diego, CA, Feb. 1992, pp. 1005-1009.

[4] Admire, J.R., Tinker, M.L. & Ivey, E.W., Mass-additive modal test method for verification of constrained structural models, *AIAA Journal*, Vol. 31, No. 11, Nov. 1993, pp. 2148-2153.

[5] Chung, Y.T., Sernaker, M.L. & Peebles, J.H., Simulating flight boundary conditions for orbiter payload modal survey, Paper No. 93-1605, *Proceedings of the AIAA/ASME/ASCE/AHS/ASC 34th Structures, Structural Dynamics and Materials Conference*, La Jolla, CA, April 1993, pp. 2624-2630.

[6] Craig, R.R., Jr., Cutshall, W.C. & Blades, E.L., *A New Substructure System Identification Method*, Report No. CAR 95-1, Center for Aeromechanics Research, The University of Texas at Austin, December 1995.

[7] Craig, R.R., Jr., Kurdila, A.J. & Kim, H.M., State-space formulation of multi-shaker modal analysis, *Int. J. Analytical and Experimental Modal Analysis*, Vol. 5, No. 3, July 1990, pp. 169-183.

[8] Leuridan, J.M., Brown, D.L. & Allemang, R.J., Direct system parameter identification of mechanical structures with application to modal analysis, Paper No. 82-0767-CP, *Proceedings of the AIAA/ASME/ASCE/AHS 23rd Structures, Structural Dynamics and Materials Conference*, New Orleans, LA, May 1982, pp. 548-556.

[9] Balmès, E., New results on the identification of normal modes from experimental complex modes, *Proceedings of the 12th International Modal Analysis Conference*, Honolulu, Hawaii, Jan.-Feb. 1994, pp. 1576-1582.

[10] Van Huffel, S. & Vandewalle, J., *The Total Least Squares Problem: Computational Aspects and Analysis*, Society of Industrial and Applied Mathematics, Philadelphia, 1991.

[11] Golub, G.H. & Van Loan, C.F., *Matrix Computations*, The Johns Hopkins University Press, Baltimore, 1983.

[12] Craig, R.R., Jr., A new substructure system identification method, *Proceedings of the 36th AIAA/ASME/ASCE/AHS/ASC Structures, Structural Dynamics, and Materials Conference*, New Orleans, LA, April 1995, pp. 1209-1217.

[13] Craig, R.R., Jr., Blades, E.L. & Cutshall, W.K., A reduced-order substructure system identification method, Paper No. AIAA-96-1200-CP, *Proceedings of the 37th AIAA Dynamics Specialists Conference, and Materials Conference*, Salt Lake City, UT, April 1996, to appear.

[14] *MATLAB*™, The MathWorks, Natick, MA, 1991.